Electroproduction of Protons at Large p_T†

A. Browman,* K. M. Hanson,* S. D. Holmes, R. V. Kline, D. Larson, F. M. Pipkin,
S. W. Raither, and A. Silverman

Laboratory for Nuclear Studies, Cornell University, Ithaca, New York 14853, and
High Energy Physics Laboratory, Harvard University, Cambridge, Massachusetts 02138
(Received 23 July 1976)

We report measurements of the inclusive electroproduction reaction $e + p \to e + p + X$ for protons produced between 100° and 150° in the virtual-photon–target-proton center-of-mass system. Data were taken at the (W, Q^2) points (2.2 GeV, 1.2 GeV^2), (2.2, 3.6), (2.65, 1.2), (2.65, 2.0), (2.65, 2.8), (2.65, 3.6), (3.1, 1.2), and (3.1, 2.0). The invariant structure function is studied as a function of W, Q^2, x_T, p_T^2, and M_X^2.

The study of hadron production at large transverse momentum is expected to yield information on the underlying structure of the hadrons.[1] Experiments completed at the CERN intersecting storage rings (ISR)[2] and at Fermi National Accelerator Laboratory (FNAL)[3] show that in purely hadronic reactions the fixed-angle behavior of the cross section is described by the form

$$(E/\sigma_T)d^3\sigma/dp^3 = f(x_T)/W^n, \quad n \sim 8 \text{ to } 11, \quad (1)$$

where $x_T = p_T/p_{max}^*$. Here p_T is the component of the momentum of the produced proton transverse to the virtual-photon direction, W is the total energy of the virtual-photon–target-proton system, p_{max}^* is the maximum kinematically allowed momentum for which the asterisk denotes the center-of-mass system. The ISR and FNAL results have been successfully interpreted through the constituent interchange model.[4]

We report here measurements of the electroproduction reaction

$$e + p \to e + p + \text{anything}, \quad (2)$$

carried out at the Wilson Synchrotron Laboratory at Cornell University. Reaction (2) is analyzed in terms of the virtual-photoproduction reaction,

$$\gamma_v + p \to p + \text{anything}, \quad (3)$$

where the square of the mass of the virtual photon $-Q^2$, energy ν, direction and polarization parameter ϵ are tagged by the scattered electron. The cross section for Reaction (2) is written,

$$d\sigma/d\Omega_e dE_e d^3p_p = \Gamma d^3\sigma/dp_p^3, \quad (4)$$

where Γ is the "flux" of virtual photons and $d^3\sigma/dp_p^3$ is the cross section for Reaction (3). The virtual photoproduction cross section is a function of W, Q^2, ϵ, x_T (or p_T, or θ), and x (or M_X^2). Here θ is the polar angle of the produced proton and M_X^2 is the square of the invariant undetected

mass. x is defined in terms of the component of the proton momentum parallel to the virtual-photon direction by $x = p_\parallel^*/p_{max}^*$. For all the data reported here $0.8 < \epsilon < 0.95$.

The data are presented in terms of the invariant structure function,

$$F = \frac{E}{\sigma_T}\frac{d^3\sigma}{dp^3} = \frac{2W}{\sigma_T p^*}\frac{d\sigma}{d\Omega_p^* dM_X^2}. \quad (5)$$

Here σ_T is the total virtual-photoproduction cross section for the W, Q^2, and ϵ of the reaction. σ_T is taken from a fit to the Stanford Linear Accelerator Center–Massachusetts Institute of Technology measurements of νW_2 with the assumption that $R = 0.18$.[5]

A two-arm spectrometer system was used to take data at the (W, Q^2) points (2.2 GeV, 1.2 GeV^2), (2.2, 3.6), (2.65, 1.2), (2.65, 2.0), (2.65, 2.8), (2.65, 3.6), (3.1, 1.2), and (3.1, 2.0). A more complete description of the apparatus appears in a previous Letter.[6] A lead-Lucite shower counter served to identify the scattered electrons. Protons were separated from pions by a threshold gas Cherenkov counter for momenta greater than 1.5 GeV/c and by time of flight at lower momenta. From an analysis of the time-of-flight spectra, the kaon contamination in the protons was estimated to be less than 3%. The data have been corrected for random coincidences (~ 1%), electronics dead time (~ 7%), target-wall background (~ 5%), absorption in the counters (~ 6%), and electron misidentification (~ 6%). The uncertainties shown are statistical only and do not include a possible systematic error estimated to be less than ± 8%. The data have not been corrected for radiative processes. A preliminary estimate of the radiative correction indicates that it is less than 15% for all the data shown.

Figure 1 shows the p_T^2 distributions for the region $-0.5 < x < -0.3$. In fitting the data to the form
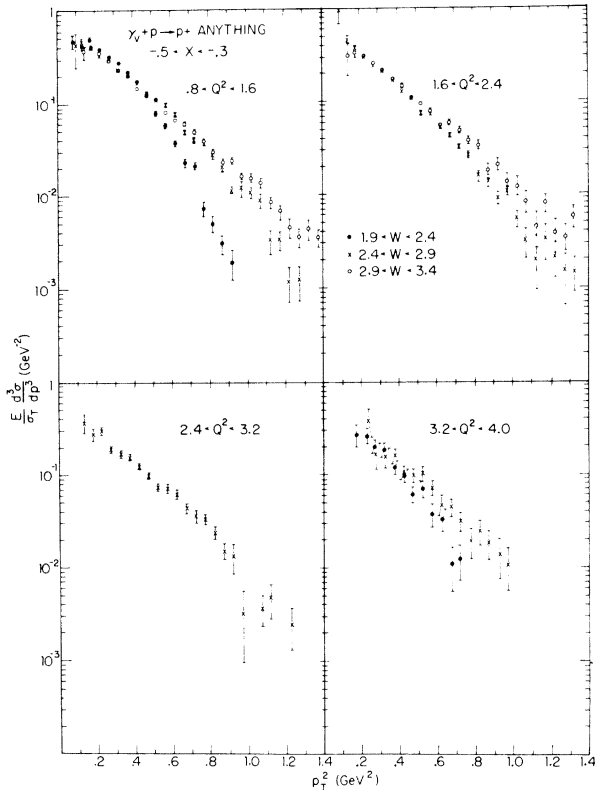
FIG. 1. The p_T^2 dependence of the invariant structure function for inclusive proton production.

$a \exp(-bp_T^2)$, we have excluded all data for which $M_X^2 < 0.75$ GeV^2 in order to stay above the masses of the known prominent resonant states. The results of the fits along with the maximum p_T^2 consistent with the constraint on the square of the missing mass are given in Table I. We have also made a single fit of all the data with M_X^2

> 0.75 GeV^2 with the simple form

$$F = a \exp(-bp_T^2)W^n (Q^2)^m, \tag{6}$$

with the result $a = 0.81 \pm 0.10$ GeV^{-2}, $b = 4.13 \pm 0.04$ GeV^{-2}, $n = 0.14 \pm 0.12$, and $m = -0.31 \pm 0.04$ [$\chi^2/$ degrees of freedom (DOF) = 161/100]. This fit indicates no W dependence and a weak Q^2 dependence. The result $b = 4.13 \pm 0.04$ GeV^{-2} agrees with the results of two other electroproduction experiments and one photoproduction experiment.[7-9]

Figure 2 shows the x_T dependence of the structure function for the eight (W, Q^2) points. This figure shows explicitly that the data do not conform to Eq. (1) and therefore do not display the scaling suggested by the hadronic data at higher energy. For $M_X^2 > 0.75$ GeV^2 and 0.8 GeV$^2 < Q^2 < 1.6$ GeV^2, a fit by Eq. (1) gives

$$n = (14.6 \pm 0.8)x_T^{2.1 \pm 0.1}. \tag{7}$$

This behavior is similar to the one found for the inclusive π^+ structure function at 90° in the center of mass.[12]

Figure 3 shows the M_X^2 dependence at fixed angle for three values of W and 0.8 GeV$^2 < Q^2 < 1.6$ GeV^2. The peak near 0.6 GeV^2 is due to the ρ meson. The data at the two higher W points have been fitted in the region $M_X^2 > 0.75$ GeV^2 with the equation

$$d\sigma/d\Omega_p^* dM_X^2 = P(M_X^2)/W^n, \tag{8}$$

where $P(M_X^2)$ is a cubic polynomial in the square of the missing mass. The fit gives $n = 12.13 \pm 0.25$ with a $\chi^2/$DOF of 97/94. The fit is shown by the solid curves in Fig. 3. The dashed curve is the fit extrapolated to 2.2 GeV. A fit to all three en-

TABLE I. Best values for a fit of the form $F = a \exp(-bp_T^2)$ for the region $-0.5 < x < -0.3$. $p_{T\,max}^2$ is the maximum p_T^2 consistent with the constraint $M_X^2 > 0.75$ GeV^2. No fit was made to the points with $W = 2.2$ GeV because the range in p_T^2 was too small to make a meaningful fit. The last column indicates the χ^2 per unit degree of freedom (DOF).

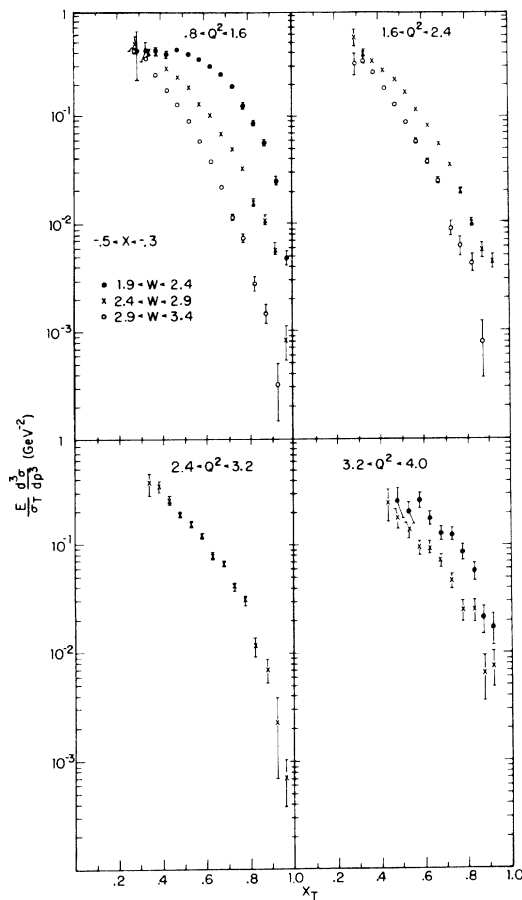| W (GeV)	Q^2 (GeV^2)	$p_{T\,max}^2$ (GeV^2)	a (GeV^{-2})	b (GeV^{-2})	$\chi^2/$DOF
2.2	1.2	0.20	•••	•••	•••
2.65	1.2	0.80	0.85 ± 0.04	4.04 ± 0.12	32/13
3.1	1.2	1.40	0.86 ± 0.02	4.06 ± 0.06	32/24
2.65	2.0	0.80	0.83 ± 0.03	4.43 ± 0.10	19/23
3.1	2.0	1.35	0.81 ± 0.04	4.11 ± 0.09	27/23
2.65	2.8	0.75	0.61 ± 0.05	3.82 ± 0.17	8/11
2.2	3.6	0.20	•••	•••	•••
2.65	3.6	0.70	0.57 ± 0.12	3.71 ± 0.42	4/8

FIG. 2. Plots of the invariant structure function versus the scaling variable x_T for the eight (W, Q^2) points.
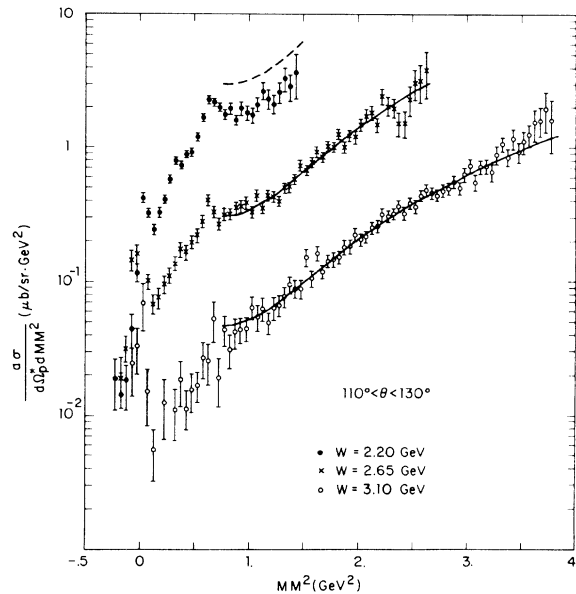

FIG. 3. $d\sigma/d\Omega_p * dM_x^2$ as a function of the square of the missing mass for $0.8 \text{ GeV}^2 < Q^2 < 1.6 \text{ GeV}$ and three values of W. The solid curves are fits by the form $d\sigma/d\Omega_p * dM_x^2 = P(M_x^2)/W^n$, where $P(M_x^2)$ is a cubic polynomial. The dashed curve is the extrapolation of this fit to $W = 2.2 \text{ GeV}$. The points near $M_x^2 = 0$ are contaminated with radiative electron-scattering events and thus do not give a reliable measurement of the reaction $\gamma_v + p \rightarrow \pi^0 + p$.

ergies gives $n = 10.64 \pm 0.22$ with the $\chi^2/\text{DOF} = 190/109$. A similar fit for the data centered on $Q^2 = 2.0 \text{ GeV}^2$ with $W = 2.65 \text{ GeV}$ and 3.1 GeV yields $n = 12.18 \pm 0.36$ with a χ^2/DOF of $82/81$. The value of n which describes the energy dependence is close to that found for π^+ mesons[10] where $n = 12.69 \pm 0.13$.

The near equality of n for the inclusive pion and proton reactions suggests that they both have a common explanation through the constituent interchange model.[1,11-13] At a fixed missing mass, the constituent interchange model suggests that the cross section should have the form

$$d\sigma/d\Omega_n * dM_x^2 = \sum_i P_i(M_x^2)/W^{2n_i - 6}, \tag{9}$$

where n_i is equal to the number of elementary fields in the ith exclusive limit channel and P is a polynomial in the square of the missing mass. For inclusive proton production two connecting

exclusive channels are[6]

$$\gamma_v + p \rightarrow \pi^0 + p, \tag{10}$$

$$\gamma_v + p \rightarrow \pi^+ + \pi^- + p. \tag{11}$$

For the first reaction, $n_i = 9$; for the second, $n_i = 11$. In the constituent interchange model each of these reactions is linked to a number of quark reactions allowed by the exchange or interchange of quark fields using the elementary two-field meson and three-field baryon wave functions. For Reaction (10) three such subreactions are

$$\gamma + (q\bar{q}) \rightarrow B + \bar{q}, \tag{12}$$

$$q + B \rightarrow B + q, \tag{13}$$

$$\gamma + B \rightarrow B + M^*. \tag{14}$$

Each of these reactions leads to a different dependence on missing mass. The data thus indicate that in this energy region both inclusive pion and inclusive proton electroproduction are dominated by reactions derived from the exclusive two-body reactions, $\gamma_v + p \rightarrow \pi^0 + p$ and $\gamma_v + p \rightarrow \pi^+ + n$.

In conclusion, we have observed that in this energy region inclusive proton production does not

exhibit the scaling behavior (1) found in purely hadronic reactions at higher energies. It is found that when the cross section is expressed in terms of the missing mass, at a fixed missing mass and fixed center-of-mass angle, the W dependence is independent of the missing mass and is the same as the one found for pion production. This behavior agrees with the predictions of the constituent interchange model indicating that the cross section is dominated by elementary quark interactions of the form of Eqs. (12)–(14). The failure to observe scaling in the form predicted by Eq. (1) may be due to the fact that no single one of the elementary quark interactions dominates in this energy region.

We wish to acknowledge the support of Professor Boyce McDaniel, the staff of the Wilson Synchrotron Laboratory, and the staff of the Harvard High Energy Physics Laboratory.

[1]D. Sivers, S. J. Brodsky, and R. Blankenbecler, Phys. Rep. 23C, 1 (1976).
[2]F. W. Busser et al., Phys. Lett. 46B, 471 (1973).
[3]J. W. Cronin et al., Phys. Rev. D 11, 3105 (1976).
[4]R. Blankenbecler, S. J. Brodsky, and J. Gunion, Phys. Rev. D 12, 3469 (1975).
[5]W. B. Atwood, private communication.
[6]A. Browman et al., Phys. Rev. Lett. 35, 1313 (1975).
[7]M. Herzlinger, Ph.D. thesis, Harvard University, 1975 (unpublished).
[8]J. C. Alder et al., Nucl. Phys. B46, 415 (1972).
[9]H. Burfeindt et al., Phys. Lett. 43B, 345 (1973).
[10]A. Browman et al., Phys. Rev. Lett. 37, 651 (1976).
[11]R. Blankenbecler, S. J. Brodsky, and J. F. Gunion, Phys. Lett. 42B, 461 (1972), and Phys. Rev. D 6, 2652 (1972).
[12]P. Landshoff and S. C. Polkinghorne, Phys. Lett. 45B, 361 (1973).
[13]R. Blankenbecler and S. J. Brodsky, Phys. Rev. D 10, 2973 (1975).

Unitary Coupled-Channel Deck Model and the Q Meson Resonance Region

J. L. Basdevant*
Fermi National Accelerator Laboratory,† Batavia, Illinois 60510

and

E. L. Berger
High Energy Physics Division,‡ Argonne National Laboratory, Argonne, Illinois 60439
(Received 17 May 1976)

We construct a unitary Deck model with coupled $K^*\pi$ and $K\rho$ channels, including only one resonance in the Q region. Adjusting the resonance parameters, we achieve a satisfactory description of the experimental phase variations and the structure in the mass spectra. The resonance is determined to belong to the $J^{PC} = 1^{+-}$ SU(3) octet, and is thus the Q_B. The relative coupling strength $K^*\pi/K\rho$ is $\sim \frac{2}{3}$.

Among the two octets of axial-vector meson resonances predicted by the quark model, only the B meson has been unambiguously identified. The apparent absence of the others is an outstanding difficulty.[1] Very recently, a Stanford Linear Accelerator Center group[2] reported evidence for the existence of two strange axial-vector mesons, Q_1 and Q_2. Their conclusion is based both on structure in the $K^*\pi$ and $K\rho$ mass distributions and on observed phase variations. In this Letter, we show that all these significant features of the data may be understood in terms of only one axial-vector resonance and nonresonant Deck

background.[3] The resonance couples to both the $K\rho$ and $K^*\pi$ channels. For reasons we describe, it must have odd charge-conjugation relative to the K. It is thus the Q_B, with $J^{PC} = 1^{+-}$. We find that its mass lies between 1.3 and 1.4 GeV, and its width is of order 150 MeV. Our description of the data without a Q_A ($J^{PC} = 1^{++}$) resonance is consistent with the apparent absence of a resonance signal in the $J^P = 1^+ \pi\rho$ A_1 system.[4]

We begin with two assumptions. First, there are nonresonant Deck amplitudes, sketched in Fig. 1, for both the $K^*\pi$ and $K\rho$ channels. Second, we assume that there is one $J^P = 1^+$ reso-